

Supporting Information

Dye Wastewater Treatment Enabled by Piezo-enhanced Photocatalysis of Single-component ZnO Nanoparticles

Yothin Chimupala¹, Chitsanupong Phromma¹, Saranphong Yimklan², Natthawat Semakul², Pipat

Ruankham^{3,4}*

¹ Department of Industrial Chemistry, Faculty of Science, Chiang Mai University, Chiang Mai,
50200, Thailand

² Department of Chemistry, Faculty of Science, Chiang Mai University, Chiang Mai, 50200,
Thailand

³ Department of Physics and Materials Science, Faculty of Science, Chiang Mai University,
Chiang Mai, 50200, Thailand

⁴ Research Center in Physics and Astronomy, Faculty of Science, Chiang Mai University, Chiang
Mai, 50200, Thailand

Table of Contents

1. Crystallinity	3
2. Size distribution of ZnO nanoparticles.....	4
3. ZnO nanoparticle formation	6
4. Electron diffraction pattern and a TEM image.....	7
5. Thermogravimetric analysis (TGA) and Differential thermal analysis (DTA).....	8
6. Brunauer–Emmett–Teller (BET) analysis	9
7. Kinetics Reaction.....	10
8. Comparison to other works	12
References	13

1. Crystallinity

Lattice parameters and crystallite size (D_{ZnO}) were calculated from the XRD spectra (Figure S1) fitted Voigt function by using Bragg's equation and Scherrer equation, respectively. The calculated values are summarized in Table S1.

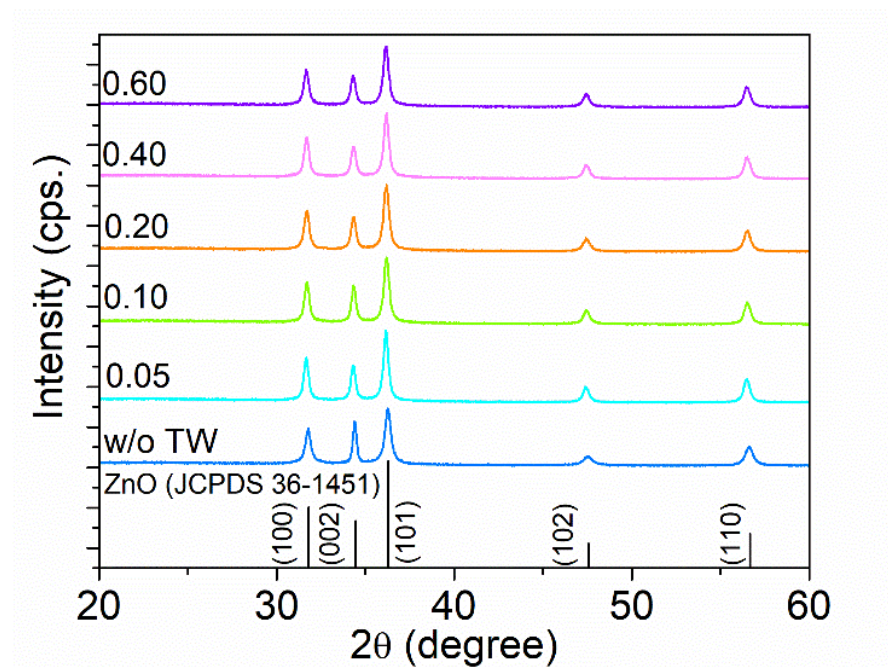


Figure S1. XRD patterns of our white precipitates synthesized using Tween80/ Zn^{2+} molar ratio at 0, 0.05, 0.10, 0.20, 0.40 and 0.60.

Table S1. Lattice parameters and crystallite size (D_{ZnO}) of the ZnO nanoparticles.

Tween80/ Zn^{2+} ratio	Lattice constant		D_{ZnO} (nm)
	a (Å)	c (Å)	
0	3.250	5.210	21.7
0.05	3.260	5.222	25.4
0.10	3.256	5.218	24.6
0.20	3.257	5.220	23.0
0.40	3.258	5.220	24.9
0.60	3.260	5.223	23.7
0.20 (calcined)	3.254	5.214	30.7

2. Size distribution of ZnO nanoparticles

Particle size distribution of ZnO nanoparticles synthesized at various Zn^{2+}/TW molar ratio was determined by image processing via ImageJ software on the observed FE-SEM images. Histograms of the samples are plotted in Figure S2.

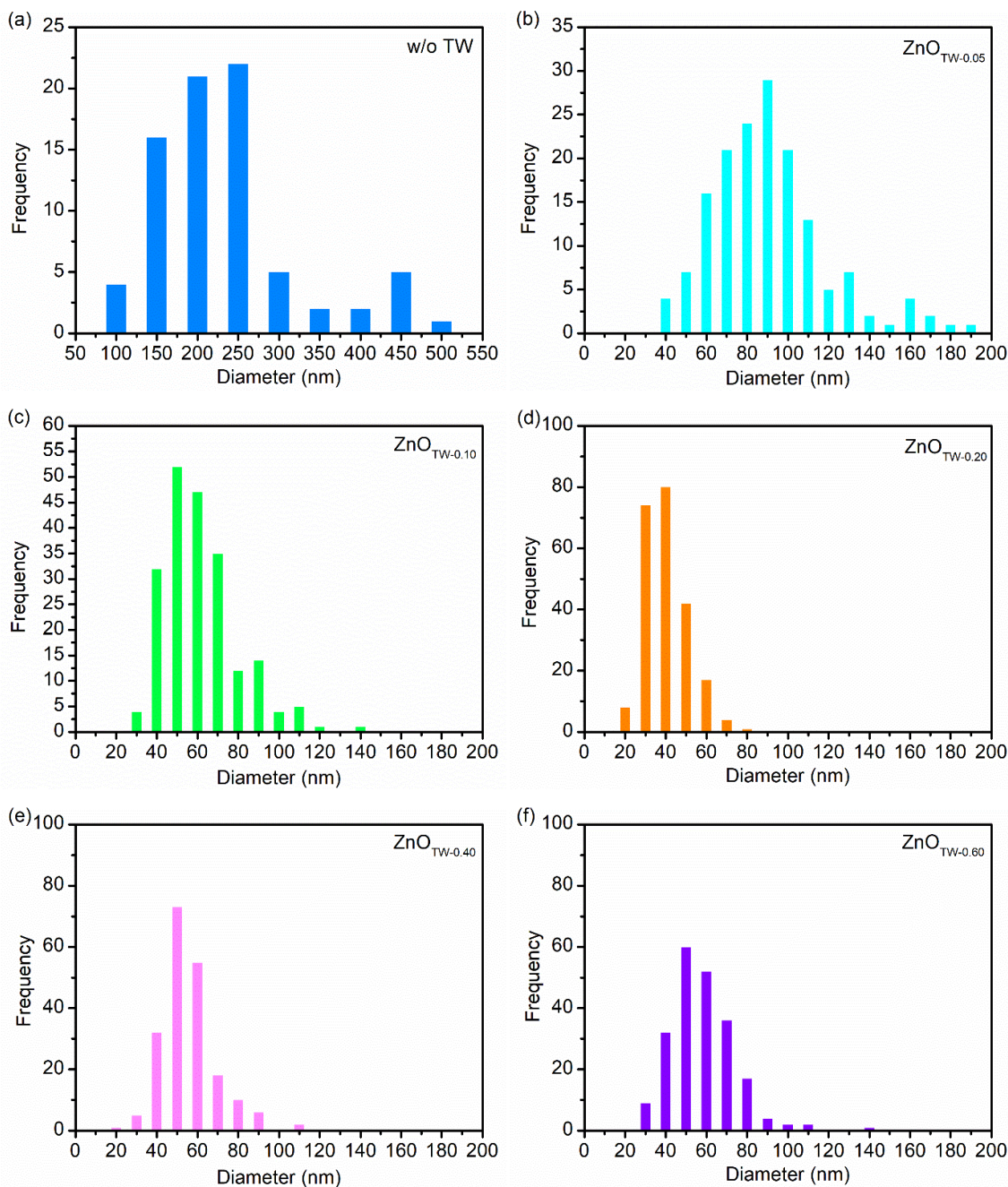


Figure S2. Size distribution histogram of (a) ZnO synthesized without TW, (b) $ZnO_{TW-0.05}$, (c) $ZnO_{TW-0.10}$, (d) $ZnO_{TW-0.20}$, (e) $ZnO_{TW-0.40}$, and (f) $ZnO_{TW-0.60}$.

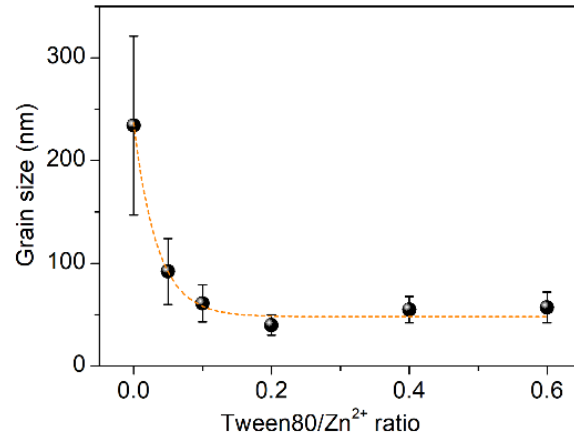


Figure S3. The semi-log plot of average grain size of ZnO nanoparticles versus TW/Zn²⁺ molar ratio used during the precipitation synthesis. Orange dash line indicates trend based on the average values.

3. ZnO nanoparticle formation

Polyoxyethylene sorbitan monooleate (or Tween 80) constitutes a large hydrophilic head (polyoxyethylene sorbitan) and small hydrophobic tail (oleate ester) as shown in Figure S4a, left. This feature makes them curvophilic (Figure S4a, right). In this way, Tween 80 molecules in aqueous solution form a micellar structure as depicted in Figure S4b. Accordingly, the complex formation between hydrophilic head (polyoxyethylene sorbitan) and Zn^{2+} ions were proposed. The addition of hydroxide into the resulting Zn^{2+} -micelle complex would generate $Zn(OH)_n$ -micelle complex. The ZnO nanoparticle formation is arguably dictated by the size of $Zn(OH)_n$ -micelle complex.

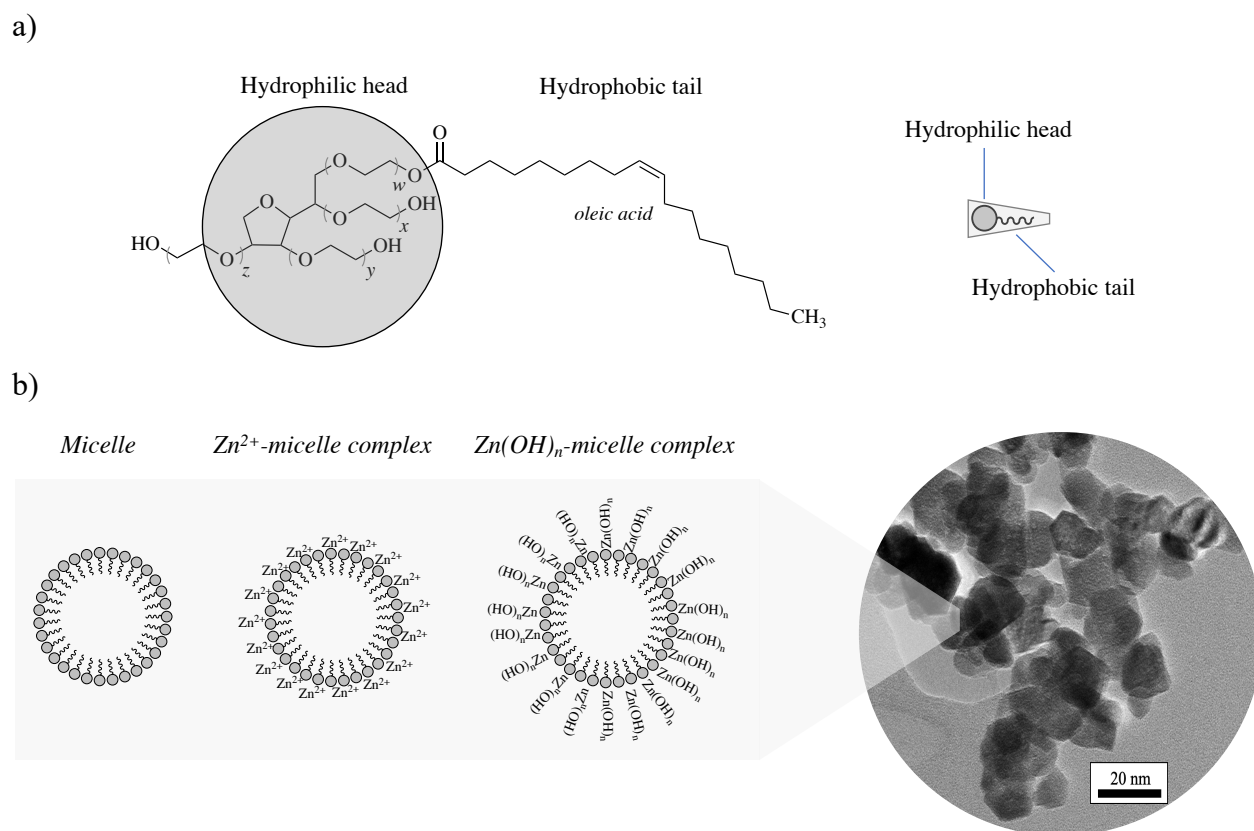


Figure S4. a) Chemical structure of polyoxyethylene (20) sorbitan monooleate (or Tween 80) and its simplified drawing of Tween 80 b) Tentative proposal for ZnO nanoparticle formation: spherical micelles in aqueous solution as a template for ZnO nanoparticle

4. Electron diffraction pattern and a TEM image

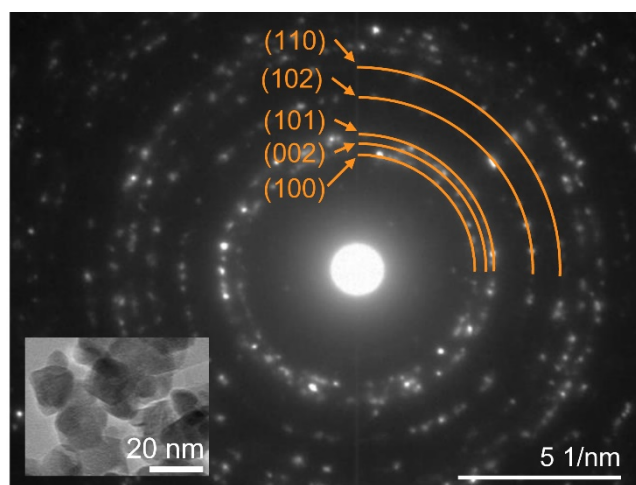


Figure S5. Electron diffraction pattern and corresponding TEM image (inset) taken from as-synthesized ZnO_{TW-0.2} nanoparticles.

5. Thermogravimetric analysis (TGA) and Differential thermal analysis (DTA)

TGA and DTA were carried out to investigate the residue percentage in the synthesized ZnO nanopowders. The TGA and DTA curves are shown in Figure S6.

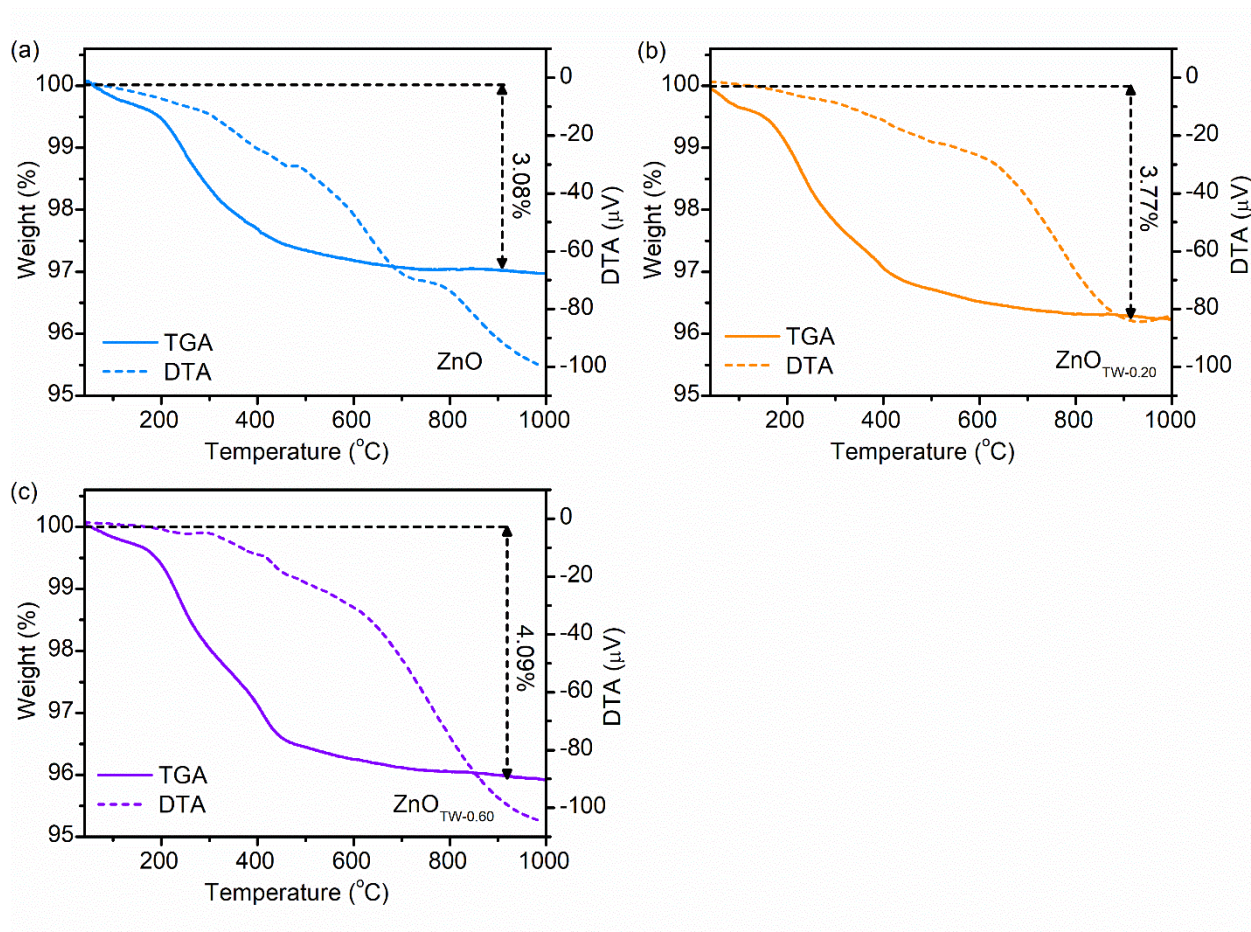


Figure S6 TGA (solid lines) and DTA (dash lines) curves of (a) ZnO_{TW-0}, (b) ZnO_{TW-0.20}, and (c) ZnO_{TW-0.60}.

6. Brunauer–Emmett–Teller (BET) analysis

N₂ adsorption–desorption isotherms (Figure S7) of ZnO and ZnO_{TW-0.20} nanopowder were measured to determine surface area and porosity. The surface area (Table S2) was calculated by using BET method.

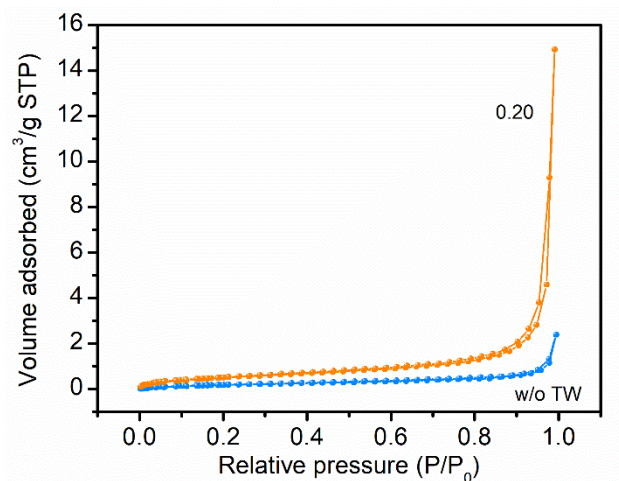


Figure S7. N₂ adsorption–desorption isotherm of ZnO powder synthesized using TW/Zn²⁺ molar ratio at 0 and 0.20.

Table S2. BET surface area of ZnO, as-synthesized ZnO_{TW-0.20}, and calcined ZnO_{TW-0.20}.

Sample	BET surface area (m ² /g)
ZnO	9.3
as-synthesized ZnO _{TW-0.20}	29.9
calcined ZnO _{TW-0.20}	20.4

7. Kinetics Reaction

The decomposition of MB dye was determined by both pseudo first-order kinetics reaction and pseudo second-order kinetics reaction in order to explain the degradation mechanism. A simplified Langmuir–Hinshelwood model¹ as presented in equation (1) was used to fit the experimental data. The equation is as follows;

$$\ln \frac{[C]}{[C_0]} = k_1 t \quad (1)$$

where k_1 is the first-order kinetics rate constant and can be extracted by the slope of a linear plot between $\ln (C/C_0)$ versus t . On the other hand, the pseudo-second-order kinetics rate constant (k_2) was evaluated by fitting the experimental data with equation (2) as follows¹;

$$\frac{1}{[C]} - \frac{1}{[C_0]} = k_2 t \quad (2)$$

The k_2 rate constant was determined from the slope of a linear plot between $1/C-1/C_0$ versus t . The extracted k_1 and k_2 values along with R-squared values are summarized in Table S3.

Table S3. The rate constants (k) of ZnO_{TW-0.20} catalysts in photocatalytic and piezo-enhanced photocatalytic activities for MB degradation using first-order and second-order kinetics fitting.

Activity	ZnO _{TW-0.20} catalysts	Dosage	First order fitting		Second order fitting	
			Rate constant (k_1 , min ⁻¹)	R ²	Rate constant (k_2 , L mg ⁻¹ min ⁻¹)	R ²
Photocatalysis	As-synthesized	0.25 g/L	0.0048	0.9702	0.0072	0.9892
		1.00 g/L	0.0055	0.9710	0.0087	0.9822
	Calcined	0.25 g/L	0.0079	0.8876	0.0140	0.9281
		1.00 g/L	0.0125	0.9192	0.0275	0.9805
Piezo- promoted photocatalysis	As-synthesized	0.25 g/L	0.0107	0.9969	0.0268	0.9538
		1.00 g/L	0.0138	0.8977	0.0502	0.9674
	Calcined	0.25 g/L	0.0123	0.9704	0.0330	0.9608
		1.00 g/L	0.0220	0.9890	0.1195	0.9392

Table S4. The rate constants (k) of ZnO_{TW-0.20} catalysts in piezo-enhanced photocatalytic activities for MB, RB and TB degradation using first-order and second-order kinetics fitting

Dyes ^{a,b}	First order fitting		Second order fitting		TOC ^c (mg/L)	
	Rate constant (k_1 , min ⁻¹)	R ²	Rate constant (k_2 , L mg ⁻¹ min ⁻¹)	R ²	Initial Concentration	After Degradation
Methylene blue (MB)	0.0220	0.9890	0.1195	0.9392	3.7	3.2
Rhodamine B (RhB)	0.0170	0.9835	0.0529	0.8837	4.9	4.3
Thymol blue (TB)	0.0155	0.9328	0.3336	0.9471	4.9	3.7

^a dye concentration is 5 ppm and ^b catalyst dosage is 1.00 g/L (200:1 by weight of ZnO:day)

^c Standard Method 5301 Total Organic Carbon (TOC)

8. Comparison to other works

The comparison of organic-dye degradation efficiency under piezo-promoted photocatalytic effect between our ZnO nanoparticles and other previously published reports is shown in Table S5. [2-7].

Table S5. Organic-dye degradation efficiency of various catalysts.

Catalyst (mg)	Dyes [†] (mg)	Catalyst: dye (wt)	Time (min)	Degradation percentage	Irradiation Condition	Vibration Condition	Ref.
ZnO nanoarrays on a steel screen (100)	MB (0.5)	200:1	50	16%	Xe lamp, 500W, 0.82 mW·cm ⁻²	Ultrasonic, (200 W)	[2]
FeS/ZnO nanoarrays on a steel screen (100)	MB (0.5)	200:1	50	97%	Xe lamp, 500W, 0.82 mW·cm ⁻²	Ultrasonic, (200 W)	[2]
Ag ₂ S@ZnO nanowires on carbon fiber cloth (N/A)	MB (0.1)	N/A	120	100%	Solar light, 320-800 nm, 186 mW·cm ⁻²	Ultrasonic, 45 kHz, (100 W)	[3]
ZnO nanowires on carbon fiber cloth (N/A)	MB (0.1)	N/A	120	88%	Solar light, 320-800 nm, 186 mW·cm ⁻²	Ultrasonic, 45 kHz, (100 W)	[3]
TiO ₂ @ZnO core-shell nanofibers (50)	MO (0.5)	100:1	120	88%	Mercury lamp, 100 W, 365 nm	Ultrasonic, 40 kHz, (120 W)	[4]
ZnO nanoparticles (N/A)	RhB (1.0)	N/A	90	70%	Xe lamp, 50 W, 30 mW·cm ⁻²	Ultrasonic, 40 kHz, (80W)	[5]
ZnO/BaTiO ₃ (N/A)	RhB (1.0)	N/A	90	100%	Xe lamp, 50 W, 30 mW·cm ⁻²	Ultrasonic, 40 kHz, (80W)	[5]
CuS/ZnO nanowires (100)	MB (0.25)	400:1	90	100%	Xe lamp, 500 W	Ultrasonic probe, (200 W)	[6]
ZnO nanotetrapods (200)	MO (0.5)	400:1	25	70%	Xe lamp, 500 W	Ultrasonic probe, (200 W)	[7]
ZnO nanoparticles (100)	MB (0.5) RhB (0.5) TB (0.5)	200:1 200:1 200:1	120 120 120	93% 90% 81%	Black light Fluorescent lamp 20 W, UVA, 365 nm, 0.94 mW·cm ⁻²	Ultrasonic bath, 40 kHz, (120W)	This work

[†]Methylene blue, methyl orange, rhodamine B and thymol blue are abbreviated for MB, MO, RhB and TB, respectively.

References

- 1 W. Gao, C. Ran, M. Wang, L. Li, Z. Sun and X. Yao, The role of reduction extent of graphene oxide in the photocatalytic performance of Ag/AgX (X = Cl, Br)/rGO composites and the pseudo-second-order kinetics reaction nature of the Ag/AgBr system, *Phys. Chem. Chem. Phys.*, 2016, **18**, 18219–18226.
- 2 X. Guo, Y. Fu, D. Hong, B. Yu, H. He, Q. Wang, L. Xing and X. Xue, High-efficiency sono-solar-induced degradation of organic dye by the piezophototronic/photocatalytic coupling effect of FeS/ZnO nanoarrays, *Nanotechnology*, 2016, **27**, 1–11.
- 3 Y. Zhang, C. Liu, G. Zhu, X. Huang, W. Liu, W. Hu, M. Song, W. He, J. Liu and J. Zhai, Piezotronic-effect-enhanced Ag₂S/ZnO photocatalyst for organic dye degradation, *RSC Adv.*, 2017, **7**, 48176–48183.
- 4 H. You, Z. Wu, Y. Jia, X. Xu, Y. Xia, Z. Han and Y. Wang, High-efficiency and mechano-/photo- bi-catalysis of piezoelectric-ZnO@ photoelectric-TiO₂ core-shell nanofibers for dye decomposition, *Chemosphere*, 2017, **183**, 528–535.
- 5 X. Zhou, S. Wu, C. Li, F. Yan, H. Bai, B. Shen, H. Zeng and J. Zhai, Piezophototronic effect in enhancing charge carrier separation and transfer in ZnO/BaTiO₃ heterostructures for high-efficiency catalytic oxidation, *Nano Energy*, 2019, **66**, 104127.
- 6 D. Hong, W. Zang, X. Guo, Y. Fu, H. He, J. Sun, L. Xing, B. Liu and X. Xue, High Piezophotocatalytic Efficiency of CuS/ZnO Nanowires Using Both Solar and Mechanical Energy for Degrading Organic Dye, *ACS Appl. Mater. Interfaces*, 2016, **8**, 21302–21314.
- 7 L. Zhang, D. Zhu, H. He, Q. Wang, L. Xing and X. Xue, Enhanced piezo/solar-photocatalytic activity of Ag/ZnO nanotetrapods arising from the coupling of surface plasmon resonance and piezophototronic effect, *J. Phys. Chem. Solids*, 2017, **102**, 27–33.